

Frequency Regulation of the Bulk Power System for Distributed Energy Resources

¹Danish Azmat Khan, ²Prof. Chetan M. Bobade

¹Research Scholar, ²Assistant Professor

^{1,2}Electrical Engineering Department,

^{1,2}G. H. Raisoni University, Amravati, India

Abstract : Due to their intermittent features and poorer inertial response, distributed energy resources (DERs) such as photovoltaic (PV) systems and fuel cell systems have increased the complexity of the power system. This reorganization of the power system has a significant impact on the system's transient responsiveness, resulting in inter-area oscillations, less synchronised coupling, and power swings. Furthermore, the idea of being dispersed and generating electricity from many points in the electrical system exacerbates the transitory impact of DERs by introducing difficulties like reverse power flows.

This technique proposed the effects of changing power system characteristics that are impeding large-scale DER integration. In addition, by introducing virtual inertia to inverter-based DERs in the electricity system, a method to enhance the system's inertial responsiveness is addressed. The suggested control increased the stability margin and allowed the system to follow its rated frequency. By increasing the rate of change of frequency, the injected synchronized active power to the system avoids the protective relays from tripping. The suggested system functioning is tested experimentally using the MATLAB 2015 simulation system on a sample power grid that includes generation, transmission, and distribution with solar pv and fuel cell system integration.

Index Terms – Frequency regulation, PQ control, VSG control.

I. INTRODUCTION

The opening of the energy market and the emergence of new circumstances in the energy sector are driving to the development of more efficient energy production and management methods. In comparison to any potential faults that the new market model may cause, the introduction of fresh ideas capable of developing in new settings may lead to more appropriate solutions.

As it advances toward a more competitive environment, the electrical industry is experiencing a massive shift. The 'growing pains' of this change - price volatility, ageing infrastructure, and shifting regulatory frameworks – are prompting both energy customers and electric utilities to reconsider the advantages of distributed generation (DG). [1] The combination of utility reorganization, technological advancements, and recent environmental regulations lays the groundwork for DG to become a viable energy source in the near future. Utility reorganization opens up energy markets, allowing customers to pick their energy provider, distribution mode, and related services. Small, modular power solutions that can be implemented quickly in response to market signals are favored by market forces.

This restructuring comes at a time when:

- Electricity demand is increasing both domestically and internationally;
- Small, modular distributed generation technologies have made significant cost and performance gains;
- Regional and global environmental concerns have placed a premium on efficiency and environmental performance; and
- Concerns have grown regarding the reliability of the grid. [2]

To enhance the sustainability of power systems, considerable inverter-based inertia-less renewable production has been incorporated in both bulk transmission and distribution (T&D) power networks in recent years. The dynamics of large-scale power networks are quickly changing due to the rising penetration of distributed energy resources (DERs) and their displacement of conventional synchronous generators (SGs). Inertia, voltage support, and oscillation damping are all lost in electric grids. When the majority of the energy is generated by synchronous generators utilizing fossil fuels, employing DERs decreases system fuel costs while also posing a substantial risk to system dependability.

Because the power electronic interfaces used in DGs lack rotational mass and dampening, the inertial constant in the microgrid is decreased, which causes the grid's rate of change of frequency (RoCoF) to increase, potentially resulting in load shedding even with minor system disruptions. The inertia of inverter-based DGs is zero. The concept of a virtual synchronous generator (VSG) has been proposed to overcome this problem, in which the power electronic interface (PEI) mimics the behavior of the SG. To stabilize the frequency, synchronized active power from the PV may be injected into the grid using the VSG method. VSG control can be separated into two portions. First, the mechanical swing equation must be numerically simulated and solved. The results are then used as a reference to adjust the inverter's voltage and current.

II. DISTRIBUTED GENERATORS

To stabilize the frequency, synchronized active power from the PV may be injected into the grid using the VSG method. VSG control can be separated into two portions. First, the mechanical swing equation must be numerically simulated and solved. The results are then used as a reference to adjust the inverter's voltage and current.

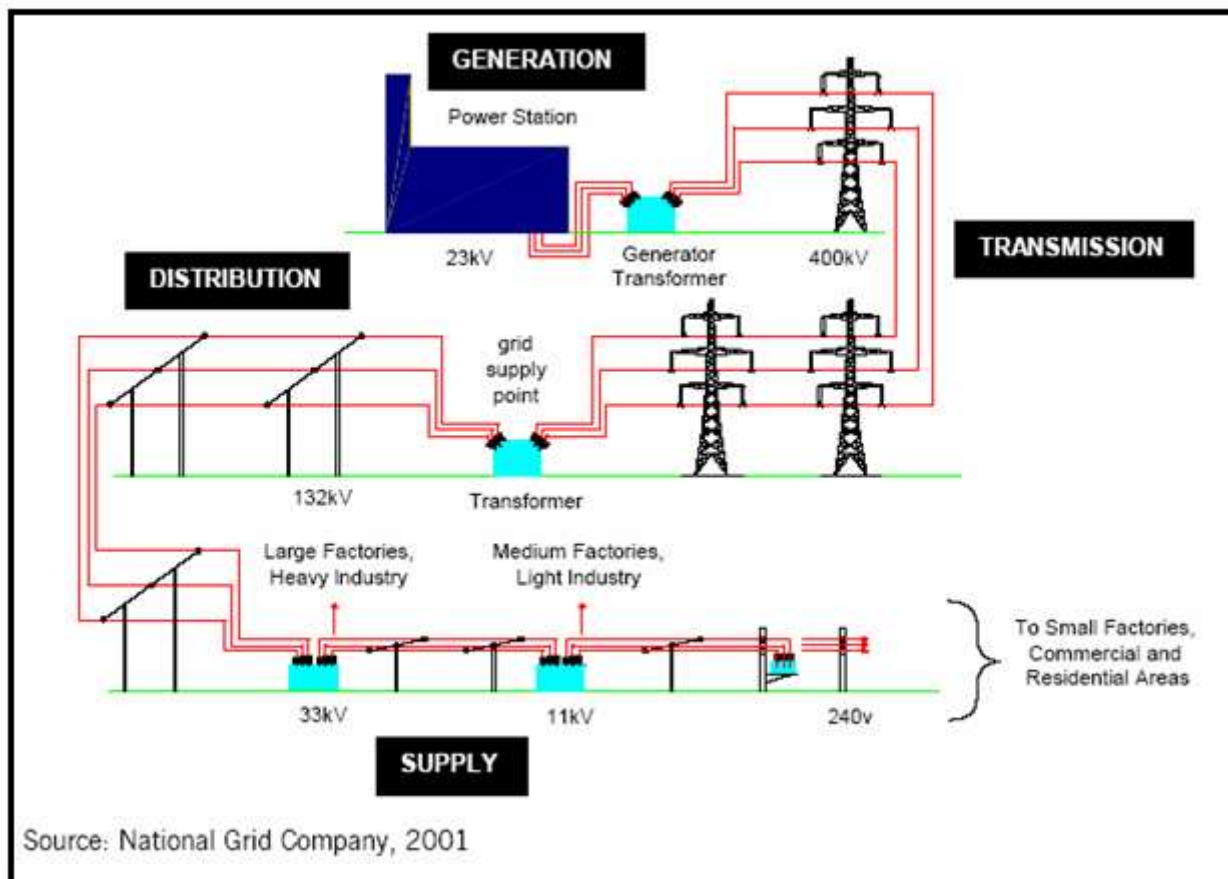


Fig.1. Line diagram of power system

The idea of distributed generation (DG) differs from traditional centralized power production, in which energy is generated in big power plants and distributed to end consumers via transmission and distribution lines (figure 1). While central power networks are still important for global energy supply, their ability to adapt to shifting energy demands is restricted. To spread energy, central power consists of big capital-intensive facilities and a transmission and distribution (T&D) system.

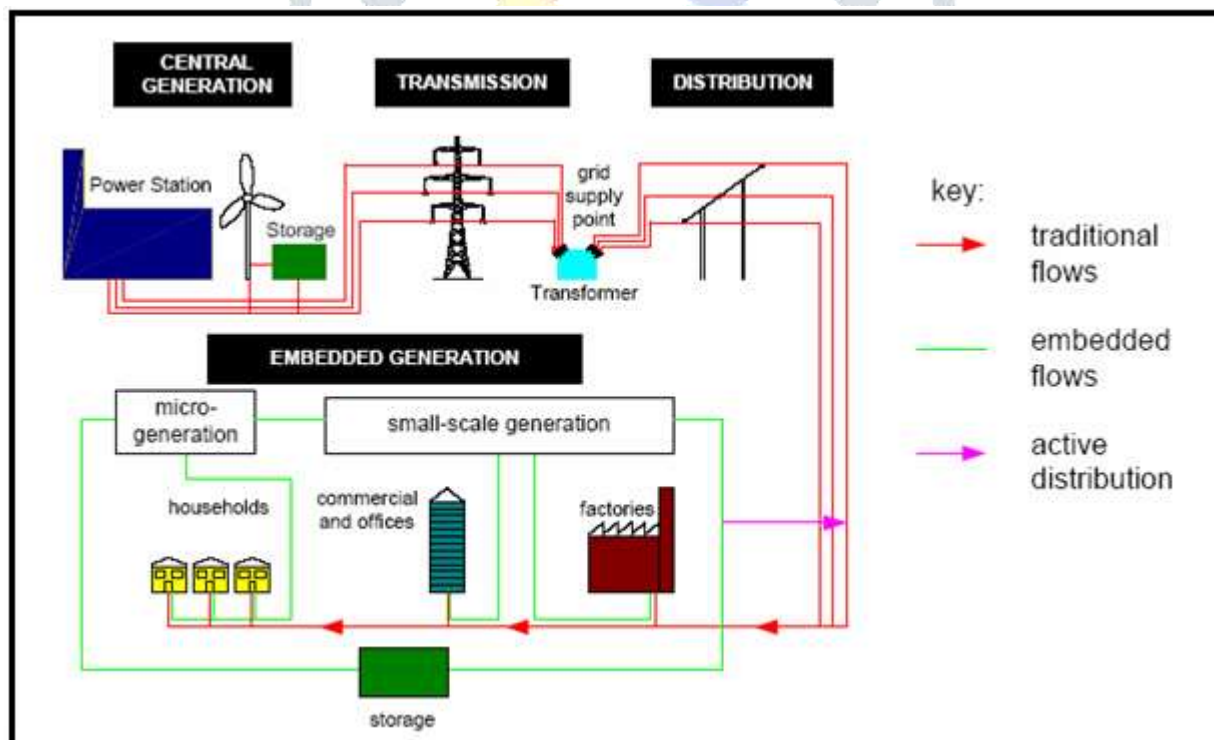


Fig.2. Distribution energy power system

In a distributed power system, small and micro generators are directly connected to factories, companies, and households, as well as lower voltage distribution networks. Electricity from directly connected users is fed into the active distribution network to meet demand elsewhere. Electricity storage technology might be used to store any extra generation. Large power plants and large-scale renewable, such as offshore wind, remain connected to the high-voltage transmission network, which ensures national backup and supply quality. Storage can be used to handle the fluctuating output of various types of generating once again. Figure 2 shows an example of a distributed electrical system.

Because of its ability to cost-effectively enhance system capacity while achieving the industry restructuring goal of market-driven, customer-oriented solutions, DG's non-traditional operating model has piqued attention. These distributed generating

systems, which can run on a variety of gas fuels; provide on-site power that is clean, efficient, dependable, and adaptable. Customers' perceptions of energy are evolving as a result of the growing range of distributed generating choices supplied by energy service providers and independent power producers.

To expand capacity, both approaches need considerable time and financial commitments. Distributed generation complements central power by (1) offering a low-cost response to incremental increases in power demand, (2) avoiding T&D capacity improvements by placing electricity where it is most required, and (3) allowing power to be returned to the grid at user locations. Significant technical advancements have resulted in significant improvements in the economic, operational, and environmental performance of tiny, modular gas-fueled power generating alternatives, thanks to decades of rigorous study. By 2030, new installed DG is expected to generate 520GW globally, according to projections. [4]

III. PROPOSED APPROACH

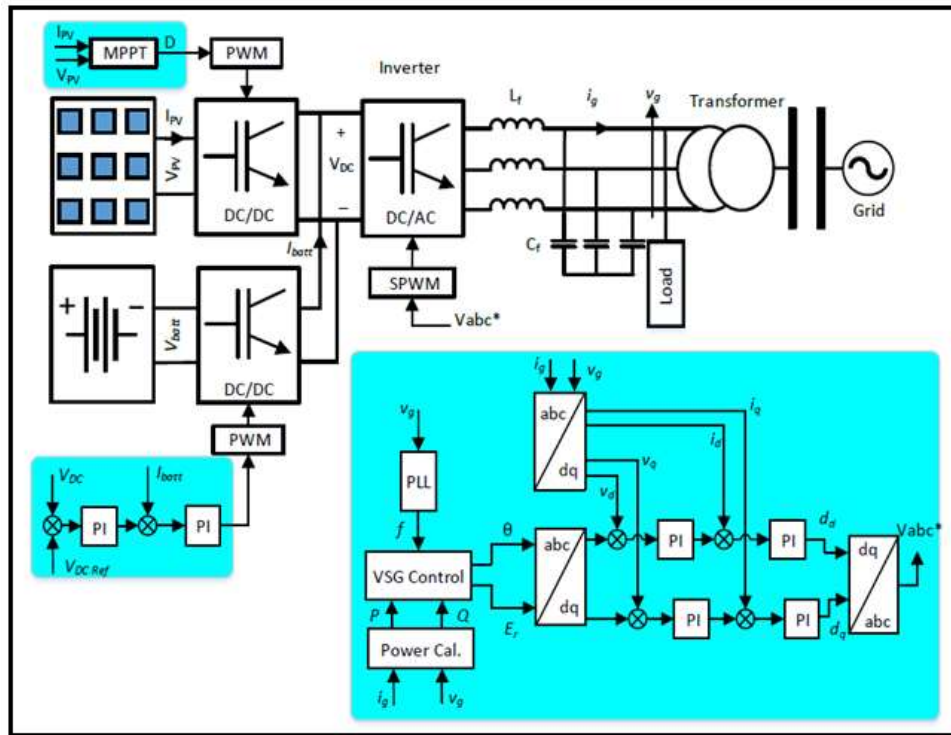


Fig.3. Complete block diagram of proposed approach

Inverters have a faster reaction time than traditional rotating machines since they don't have any mechanical rotational parts [10]. The notion of virtual inertia is proposed as a way to circumvent this restriction [11]. Similar behavior may be anticipated during regular operation of the system and frequency disturbances, such as when there is a rapid shift (increase or reduction) in active power, by simulating the mechanical equation of a genuine synchronous generator into the inverter. To stabilize the frequency, synchronized active power may be injected from the PV to the grid using the VSG algorithm [12], [13].

The perturb and observe technique (P&O) determines the active power reference P_{ref} by monitoring voltage and current of the PV during normal operation of the system (rated frequency and voltage) [28]. As illustrated in Fig. 3, the active power is regulated in two phases. Primary frequency is applied in the same way as an SG in the first step. To complete the loop, virtual inertia and damping are introduced in the second stage. As a consequence, a reference angle is created, which will be supplied into park transform [14]. The VSG control system is separated into two parts. First, the mechanical swing equation must be numerically simulated and solved. The results are then used as a reference to adjust the inverter's voltage and current.

IV. MATLAB SIMULATION MODEL

A. Solar PV Array Subsystem

Figure 4 depicts the Suntech solar pv 285 W module specification that was used in the system design. Figure 6.3 also depicts the typical manufacturing PV and VI parameters for the Suntech 285 W solar pv module under various solar irradiation conditions. Solar pv module is designed in matlab simulink modelling and analysis for varied solar irradiation according to name plate specifications. PV and VI characteristics are seen with irradiation ranging from 100 W/m² to 1000 W/m².



Electrical Characteristics

STC	STP285-20/ Wfh	STP280-20/ Wfh	STP275-20/ Wfh
Maximum Power at STC (Pmax)	285 W	280 W	275 W
Optimum Operating Voltage (Vmp)	31.4 V	31.2 V	31.1 V
Optimum Operating Current (Imp)	9.08 A	8.98 A	8.85 A
Open Circuit Voltage (Voc)	38.3 V ±5%	38.1 V ±5%	38.0 V ±5%
Short Circuit Current (Isc)	9.48 A ±5%	9.37 A ±5%	9.24 A ±5%
Module Efficiency	17.2%	16.9%	16.6%
Operating Module Temperature	-40 °C to +85 °C		
Maximum System Voltage	1000 V DC (IEC)		
Maximum Series Fuse Rating	20 A		
Power Tolerance	0/+5 W		

STC: Irradiance 1000 W/m², module temperature 25 °C, AM=1.5;
 Test in Class AAA solar simulator (IEC 60904-9) used, power measurement uncertainty is within +/- 3%

Fig.4. Electrical Characteristics of 285 W solar PV module (SUNTECH Manufacturer ratings)

Table.1. Solar pv module specification

Electrical Specification	Values
Module efficiency	14.7%
Power output tolerance	+/-3%
Maximum power voltage	35.6 V
Maximum power current	8.02 A
Open circuit voltage Voc	44.7 V
Short circuit current Isc	8.5 A
Peak power Pmax	285 W

Although there are many different types of solar cell materials, silicon is now the most used owing to its scalability, momentum, and light absorption efficiency. The stationary PV array must be at least 5kW in size. This PV array has 16 modules since each string has four modules linked in series and four strings connected in parallel. As illustrated in figure 4, each 285W solar panel has 36 PV cells linked in series. Table 1 lists the characteristics of the solar module under investigation.

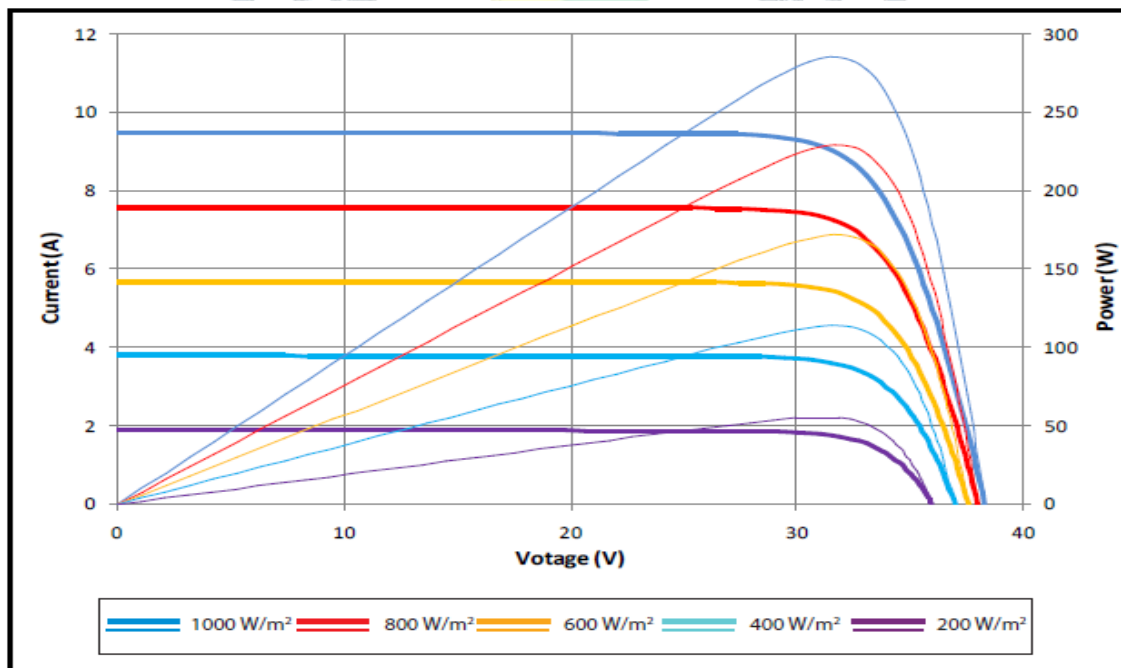


Fig.5. Standard VI and PV characteristics of SUNTECH 285 W solar PV module at different irradiances

Figure 5 depicts the Suntech solar pv 285 W module specification that was used in the system design. Figure 4 also depicts the typical manufacturing PV and VI parameters for the Suntech 285 W solar pv module under various solar irradiation conditions. Solar pv module is designed in matlab simulink modeling and analysis for varied solar irradiation according to name plate specifications. PV and VI characteristics are seen with irradiation ranging from 100 W/m² to 1000 W/m².

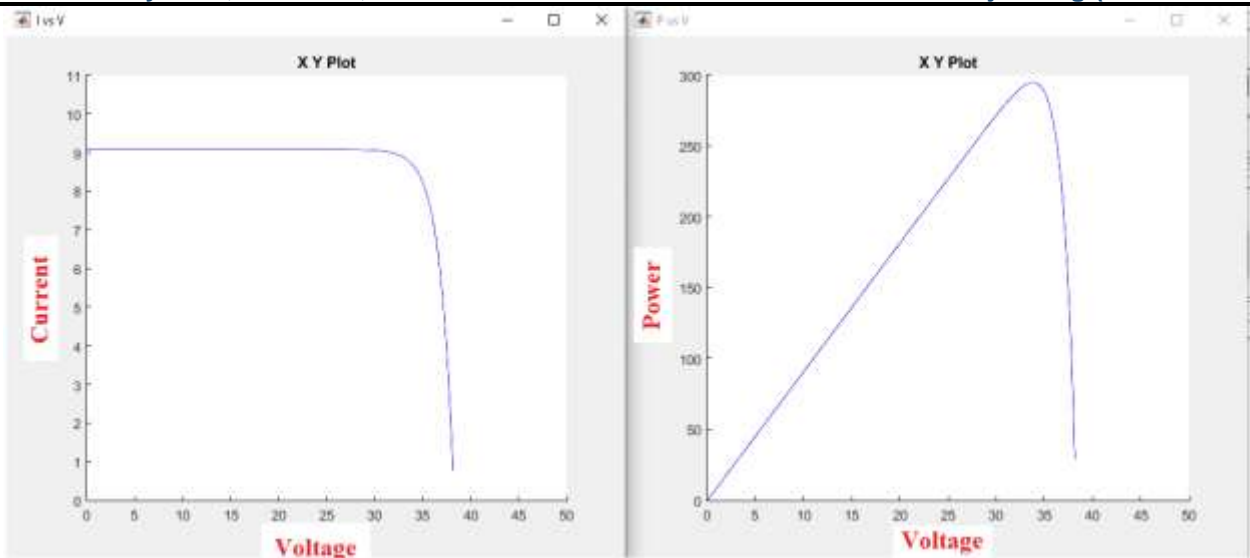


Fig.5. VI and PV characteristics of SUNTECH 285 W solar PV module at 1000 W/m² irradiation using MATLAB simulink modeling

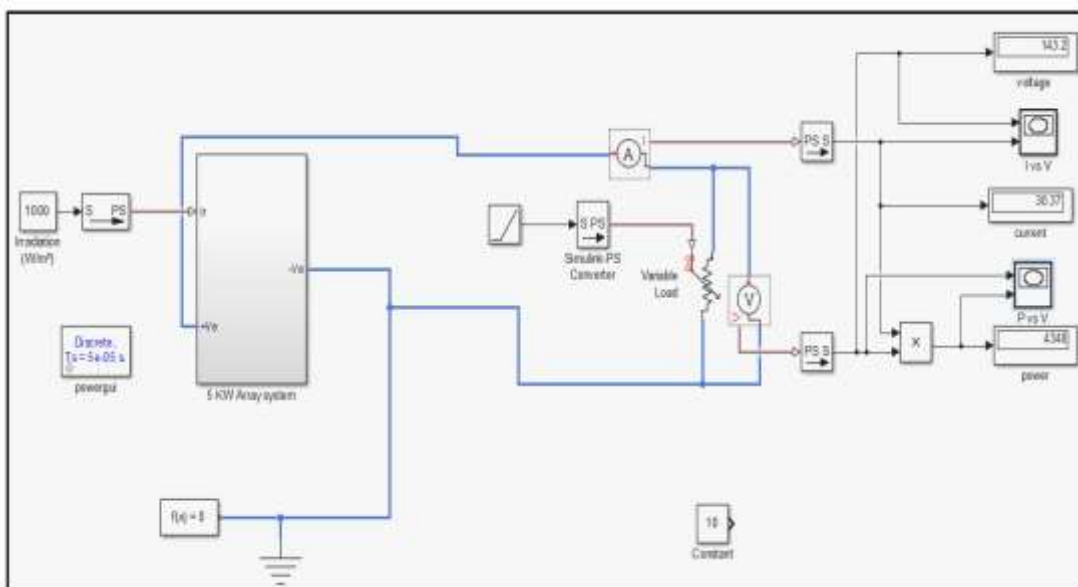


Fig.6. MATLAB simulink model of 5KW solar pv array system for VI and PV characteristics calibration

Table.2. Specification of 5KW solar array system

Parameters	Specification
Module manufacture with model code	SUNTECH STP285-20/Wfh
Power output of PV Module	285 W
Module voltage (Voc)	38.3 V
Module short circuit current (Isc)	9.08 A
Number of series connected modules per string	4 Nos
Number of parallel connected strings	4 Nos

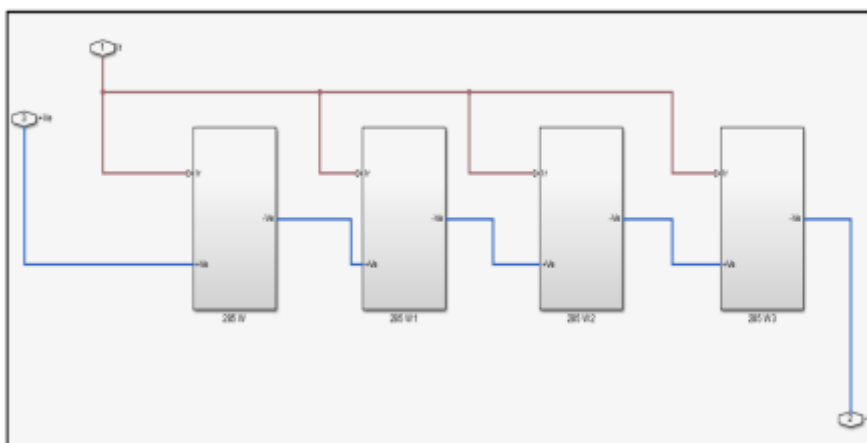


Fig.7. MATLAB simulink model of series connected string-1 subsystem in 5 KW solar array systems

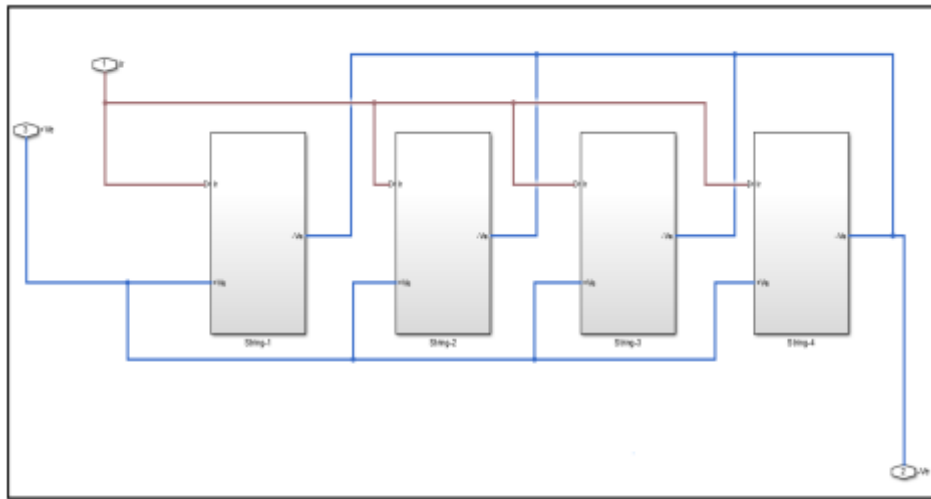


Fig.8. MATLAB simulink model of parallel connected all solar strings subsystem in 5 KW solar array systems

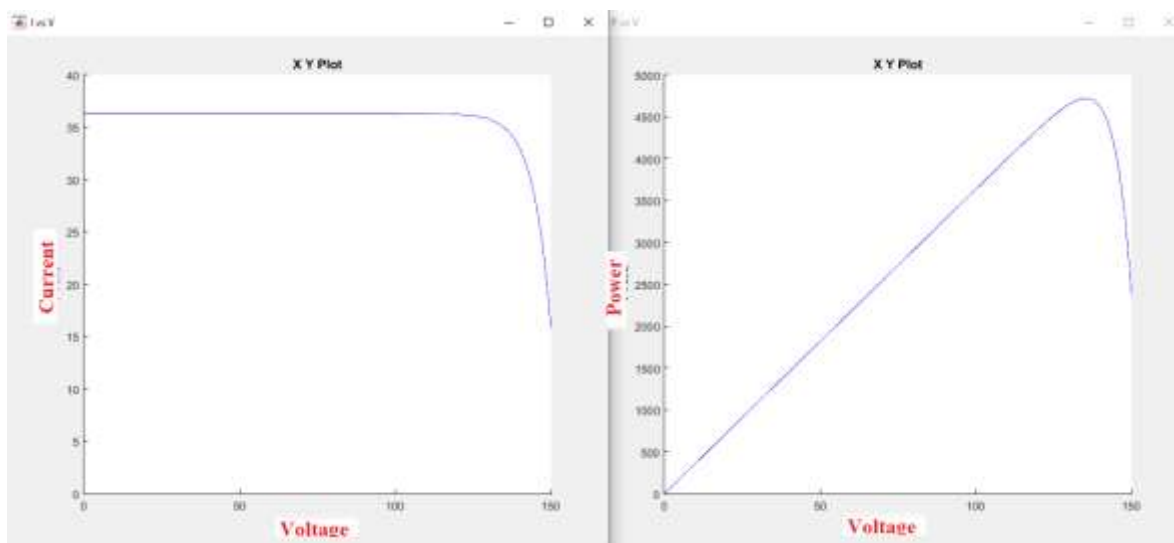


Fig.9. VI and PV characteristics of 5 KW solar PV array at 1000 W/m² irradiation using MATLAB simulink modeling

Figure 9 shows the VI and PV characteristics of 5 KW solar PV array at 1000 W/m² irradiation in which here it is observe that, peak power generated is 4800 W and maximum current achieved 37 Amp at 150 Volts voltage.

Block Parameters: PV Array

PV array (mask) (link)

Implements a PV array built of strings of PV modules connected in parallel. Each string consists of modules connected in series. Allows modeling of a variety of preset PV modules available from NREL System Advisor Model (Jan. 2014) as well as user-defined PV module.

Input 1 = Sun irradiance, in W/m², and input 2 = Cell temperature, in deg.C.

Parameters **Advanced**

Array data

Parallel strings:

Series-connected modules per string:

Module data

Module:

Plot I-V and P-V characteristics when a module is selected

Maximum Power (W): <input type="text" value="213.15"/>	Cells per module (Ncell): <input type="text" value="60"/>
Open circuit voltage Voc (V): <input type="text" value="36.3"/>	Short-circuit current Isc (A): <input type="text" value="7.84"/>

Model parameters

Light-generated current IL (A):

Diode saturation current I0 (A):

Diode ideality factor:

Display I-V and P-V characteristics of ...:

Irradiances (W/m²):

Fig.10. MATLAB simulink specification window of model of solar pv array system

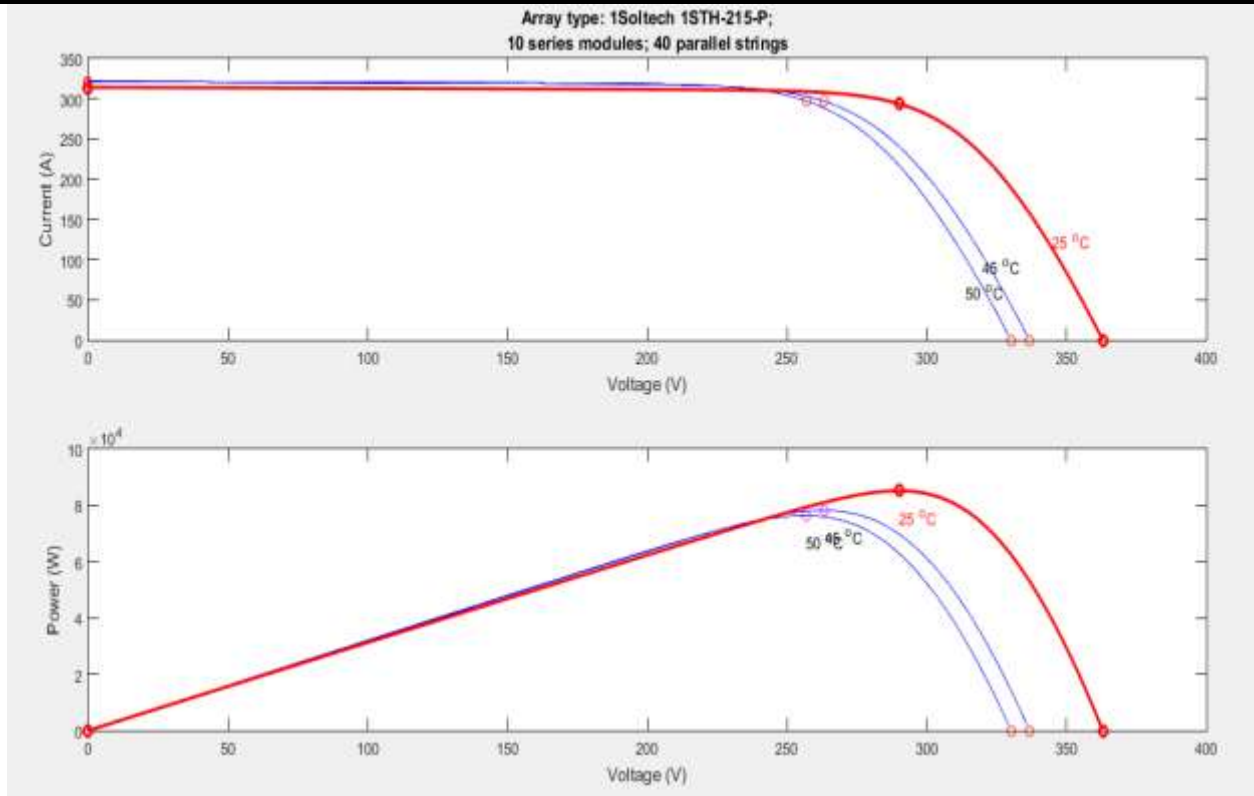


Fig.11. Solar PV and VI characteristics of single PV array at 1000 w/m2 solar irradiation for different temperature.

B. Fuel cell battery subsystem

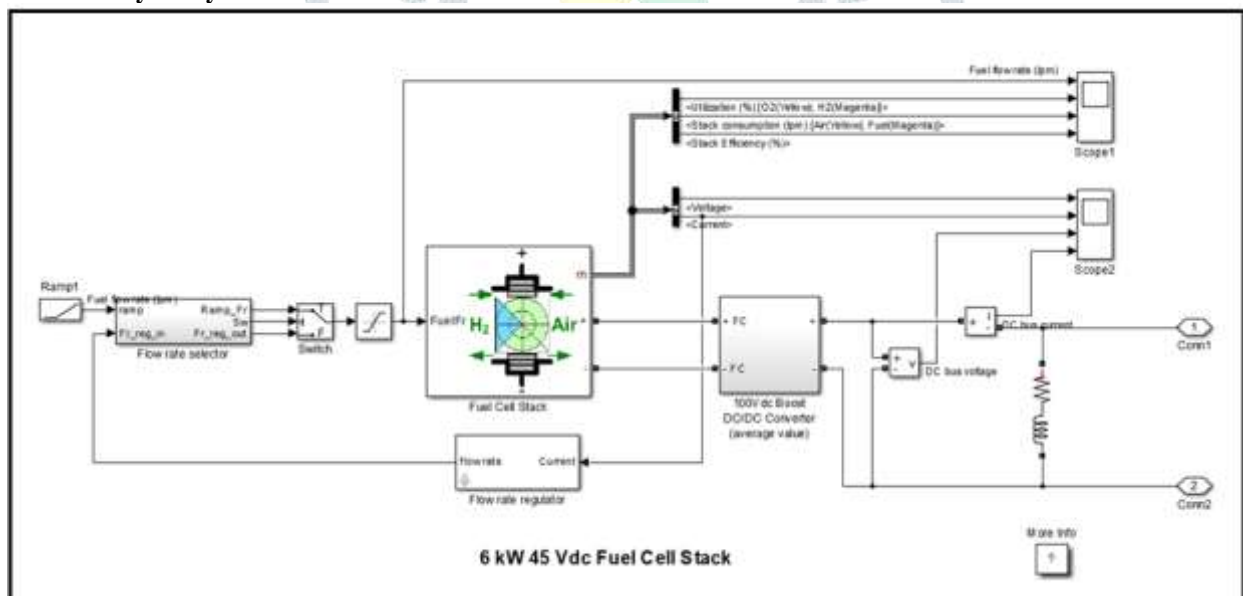


Fig.12. Fuel cell battery system matlab simulink model

Table.3. Parameter specification of fuel cell battery subsystem model

Sr No	Name of simulation block	Specification
1.	Fuel cell stack	Type of fuel cell: Proton Exchange Membrane Fuel Cell (PEMEC) (6KW, 45 Vdc) Normal operating point current $I_{nom}=133.33A$, $V_{nom}=45V$, Maximum operating point current $I_{end}=225A$, Maximum operating point voltage $V_{end}=37 V$, Number of cells = 65, Nominal stack efficiency = 55%, Operating temperature = 65 Degree, Nominal air flow rate (I_{pm}) = 300.
2.	MOSFET	FET resistance $R_{on} = 0.1 \text{ Ohm}$, Internal diode inductance $L_{on}=0 \text{ H}$, Internal diode resistance $R_d=0.01 \text{ Ohm}$, Internal diode forward voltage $V_f = 0 \text{ V}$, Snubber resistance $R_s= 100 \text{ Kohm}$, Snubber capacitor $C_s=Infinite$
3.	IGBT (Inverter)	Resistance $R_{on} = 0.001 \text{ Ohm}$, Inductance $L_{on} = 0 \text{ H}$, Forward voltage $V_f = 1 \text{ V}$, Current fall time $T_f = 1 \text{ Micro-Second}$, Current tail time $T_t = 2 \text{ Micro-Second}$, Snubber resistance $R_s = 100 \text{ Kohm}$, Snubber capacitor $C_s = Infinite$

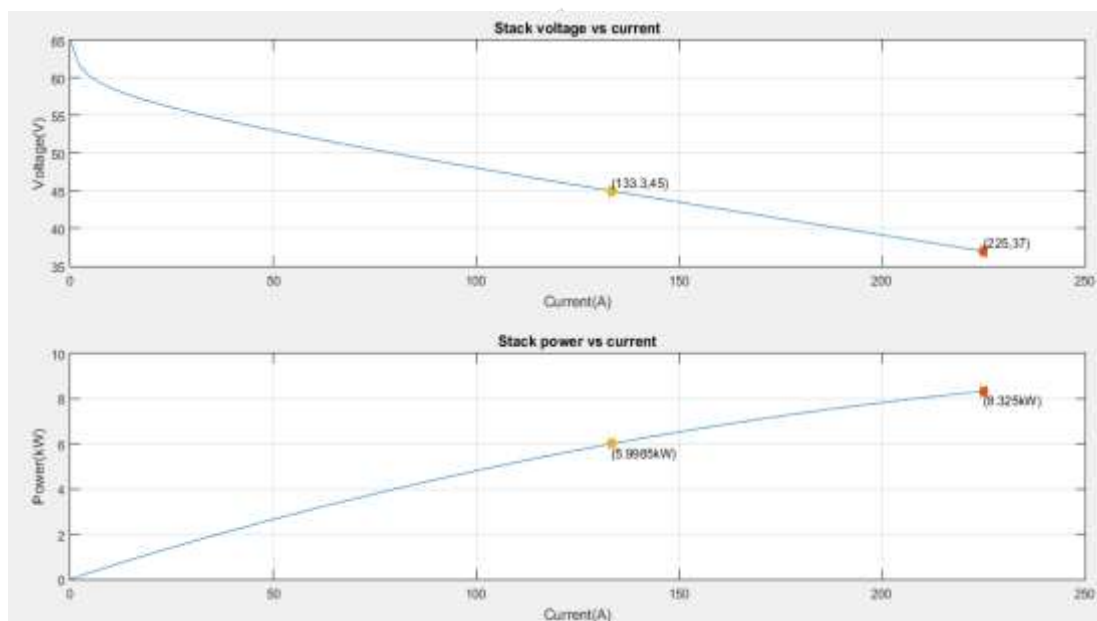


Fig.13. VI Characteristics of fuel cell

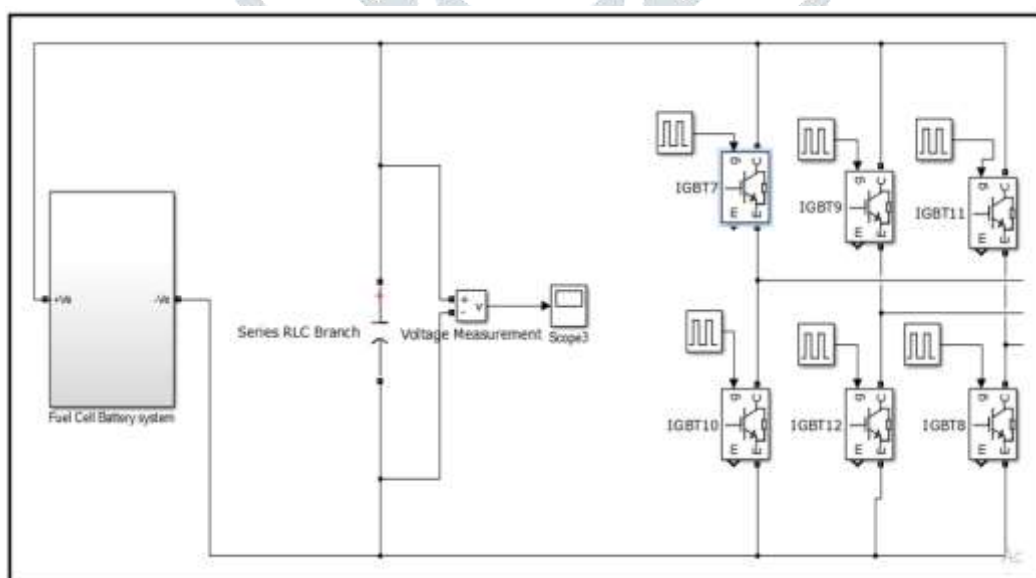


Fig.14. Three phase inverter subsystem in fuel cell subsystem

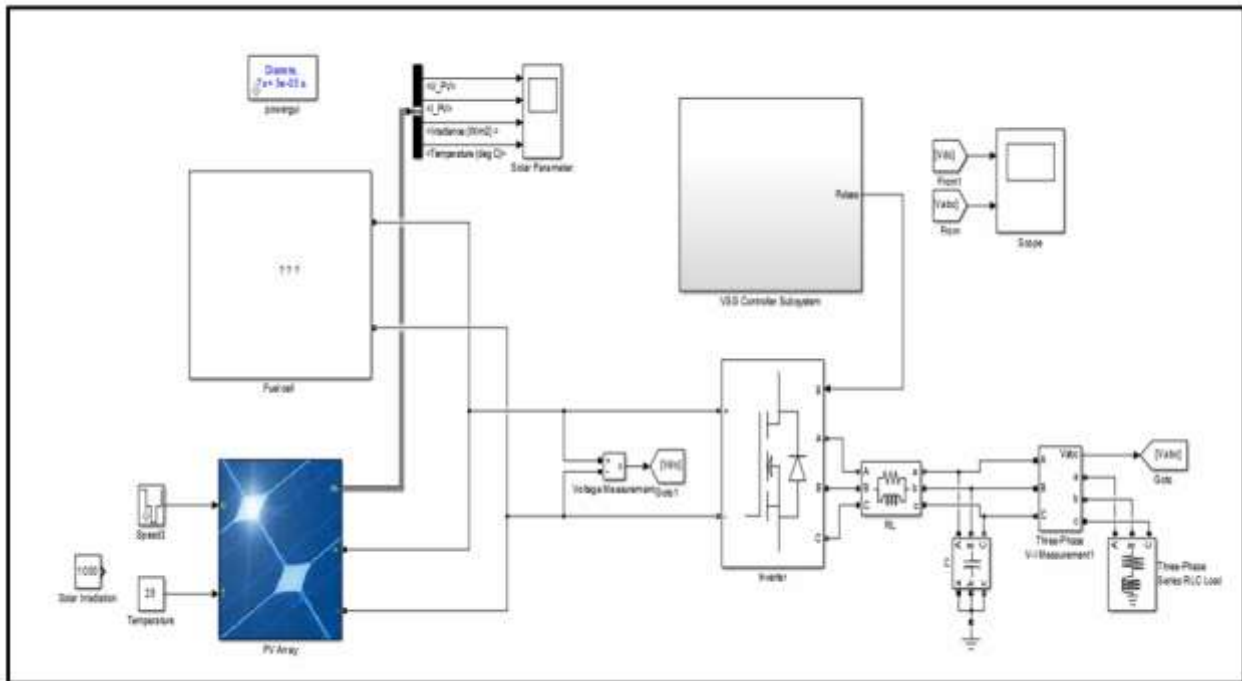


Fig.15. Complete matlab simulation model

Table.4. Simulation model parameter for pulse generator of inverter system

Sr. No.	Name of simulation block	Specification
1.	Pulse generator for IGBT-1	Pulse type = Time based, Amplitude = 1; Period = 20 Mili-second, Pulse Width = 50%, Phase delay = 0 Sec
2.	Pulse generator for IGBT-2	Pulse type = Time based, Amplitude = 1; Period = 20 Mili-second, Pulse Width = 50%, Phase delay = 3.33 Mili-Sec
3.	Pulse generator for IGBT-3	Pulse type = Time based, Amplitude = 1; Period = 20 Mili-second, Pulse Width = 50%, Phase delay = 6.667 Mili-Sec
4.	Pulse generator for IGBT-4	Pulse type = Time based, Amplitude = 1; Period = 20 Mili-second, Pulse Width = 50%, Phase delay = 10 Mili-Sec
5.	Pulse generator for IGBT-5	Pulse type = Time based, Amplitude = 1; Period = 20 Mili-second, Pulse Width = 50%, Phase delay = -6.667 Mili-Sec
6.	Pulse generator for IGBT-6	Pulse type = Time based, Amplitude = 1; Period = 20 Mili-second, Pulse Width = 50%, Phase delay = -3.33 Mili-Sec

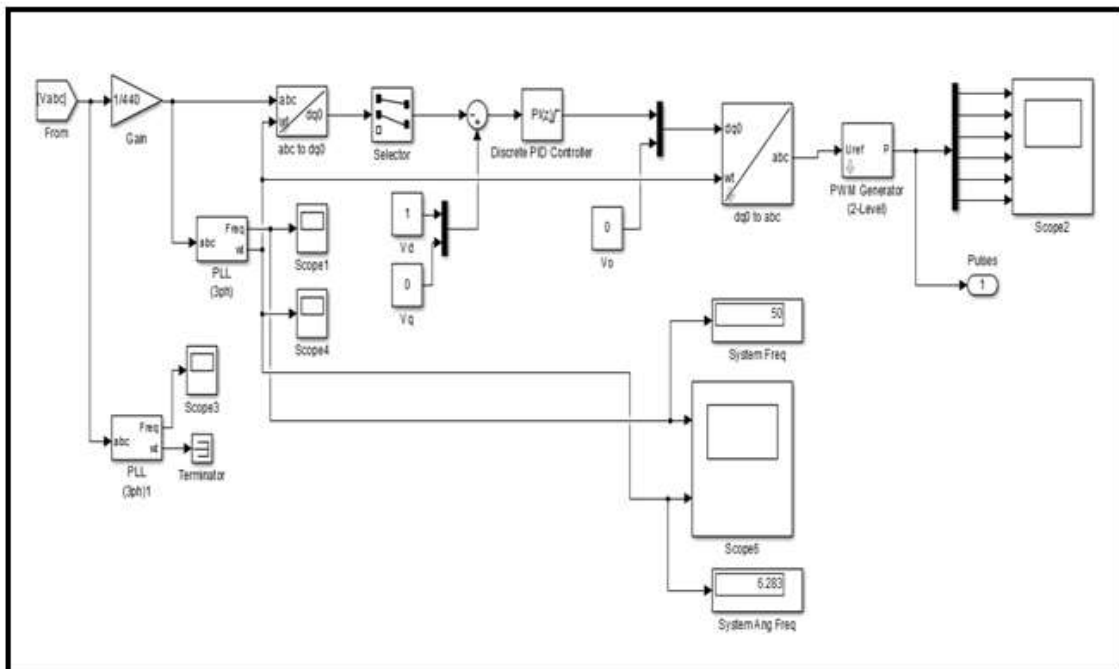


Fig.16. VSG controller subsystem model design in MATLAB simulation

V. SIMULATION RESULTS

A. Case-2: Variable fuel flow rate and constant solar irradiation

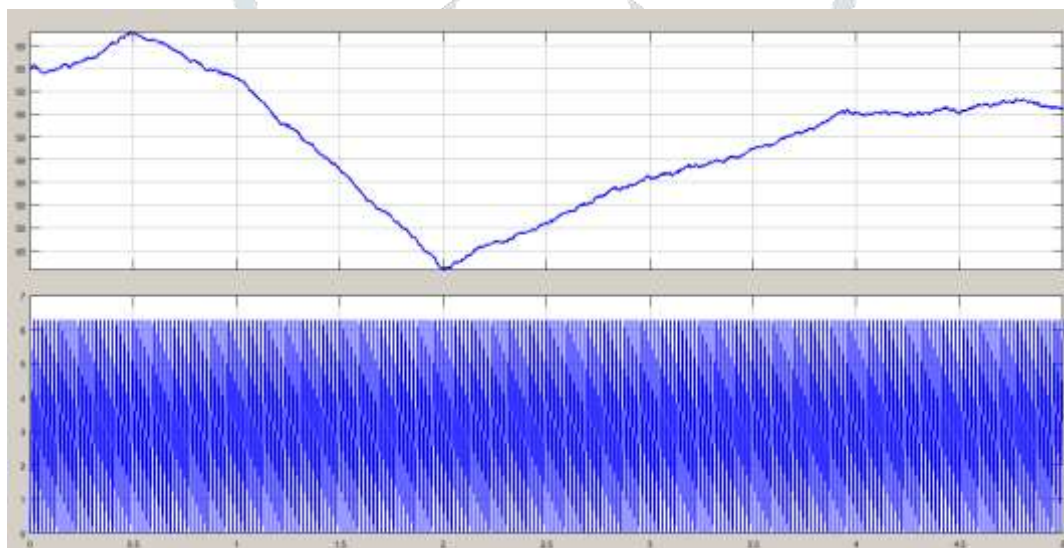


Fig.19. Frequency of system and angular frequency of power system during normal condition (Constant solar irradiation and constant fuel flow rate) case-1

Figure 19 shows the supply frequency in Hz and angular frequency of power system in rad/sec during case-1 i.e. constant solar irradiation and constant fuel flow rate. Here it is observe that, supply frequency is constant throughout the operation that is 50 Hz. Where, before 1.5 second simulation time, small fluctuation present in power system frequency which is negligible.

Figure 20 shows the Solar PV output DC voltage, Output DC Current, solar irradiation and temperature during case-1. Here it is observe that, Solar PV output voltage becomes 220 Volts and solar PV current becomes 310 Amp constant throughout the operation. Also solar irradiation becomes 1000 W/m² and solar temperature becomes 25 degree Celsius constant throughout the operation under case-1.

Figure 21 shows the output DC voltage, DC current, DC generated voltage and DC bus generated current of fuel cell system during case-1. Here, it is observed that, dc output voltage is 70V, fuel system current becomes 5 Amp, DC bus voltage becomes 230 V and DC bus current becomes 100 Amp during case-1.

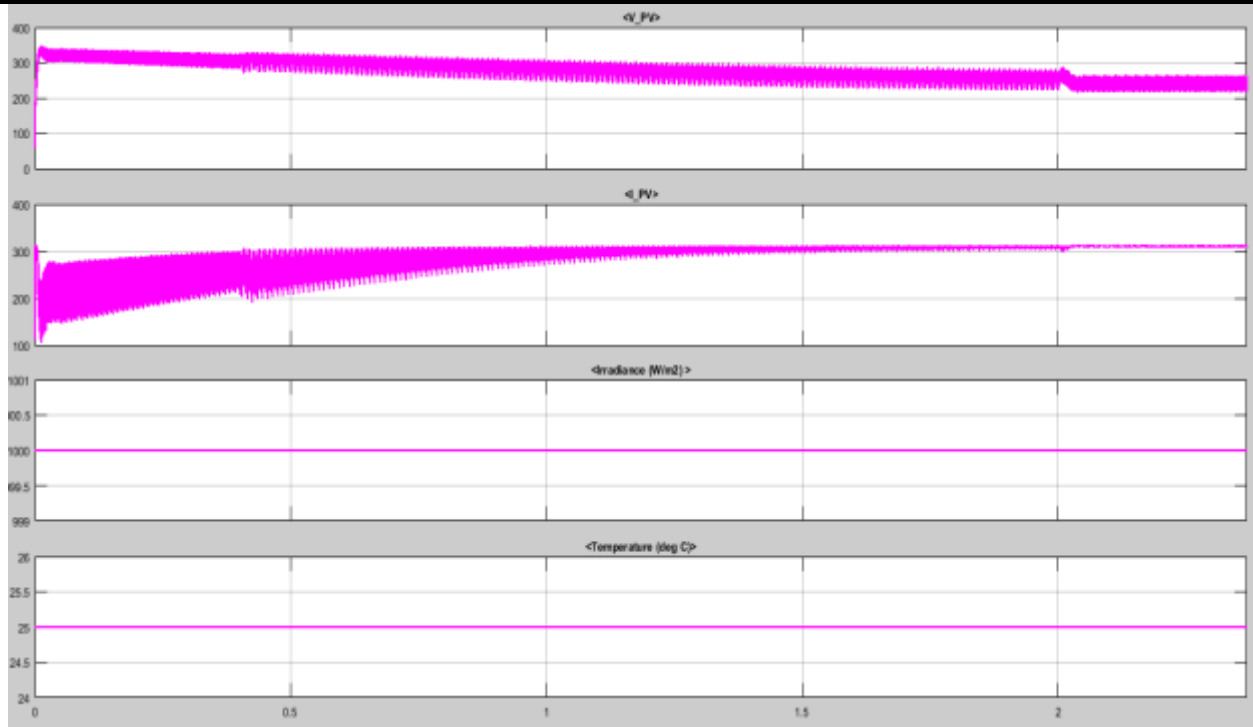


Fig.20. Solar PV output DC voltage, Output DC Current, solar irradiation and temperature during case-1

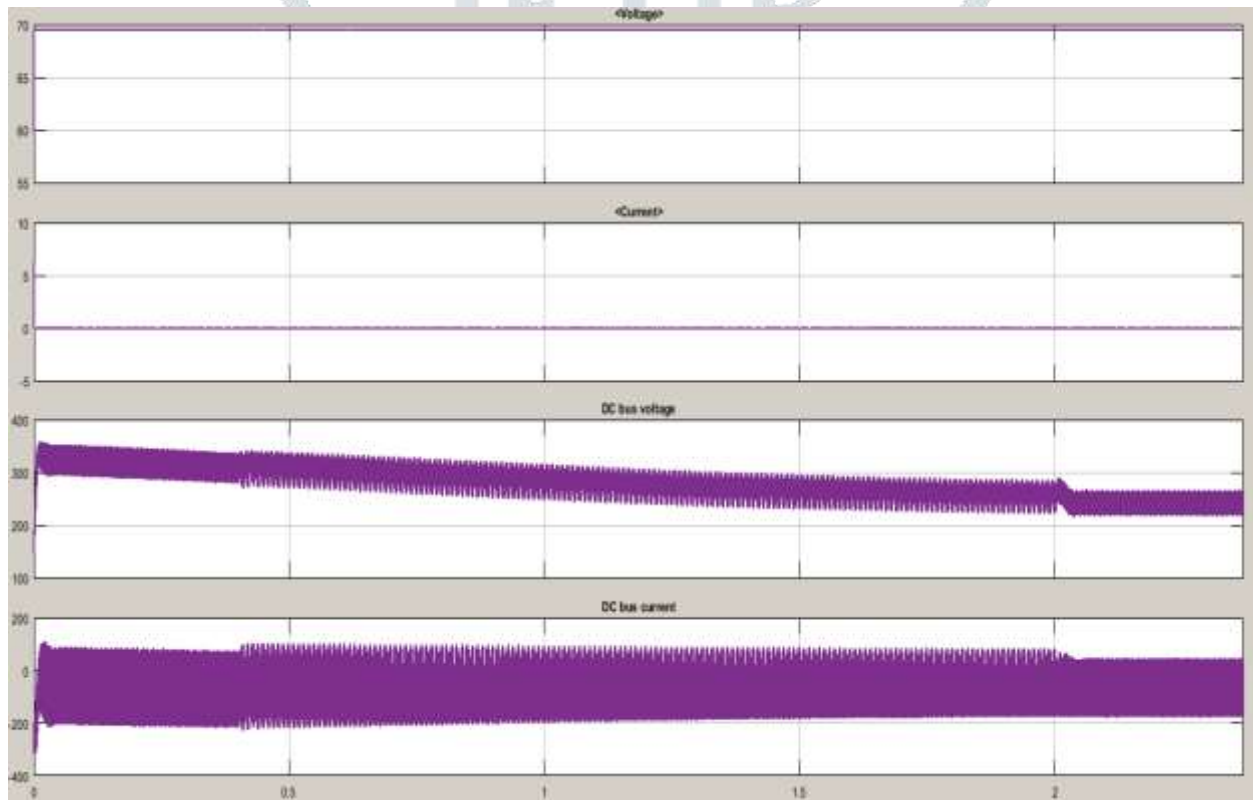


Fig.21. Output DC Voltage, dc current, dc bus generated voltage and dc bus generated current of fuel system during case-1

B. Case-2: Variable fuel flow rate and constant solar irradiation

Figure 22 shows the DC output voltage of solar pv system and lower Y-axis represent the three phase RMS voltage during normal condition. Here it is observe that, from 0.5 to 2 sec simulation time, there is some fluctuation called as transient period. Then after transient period, the output DC voltage and AC generated voltage become constant and rated without any fluctuations.

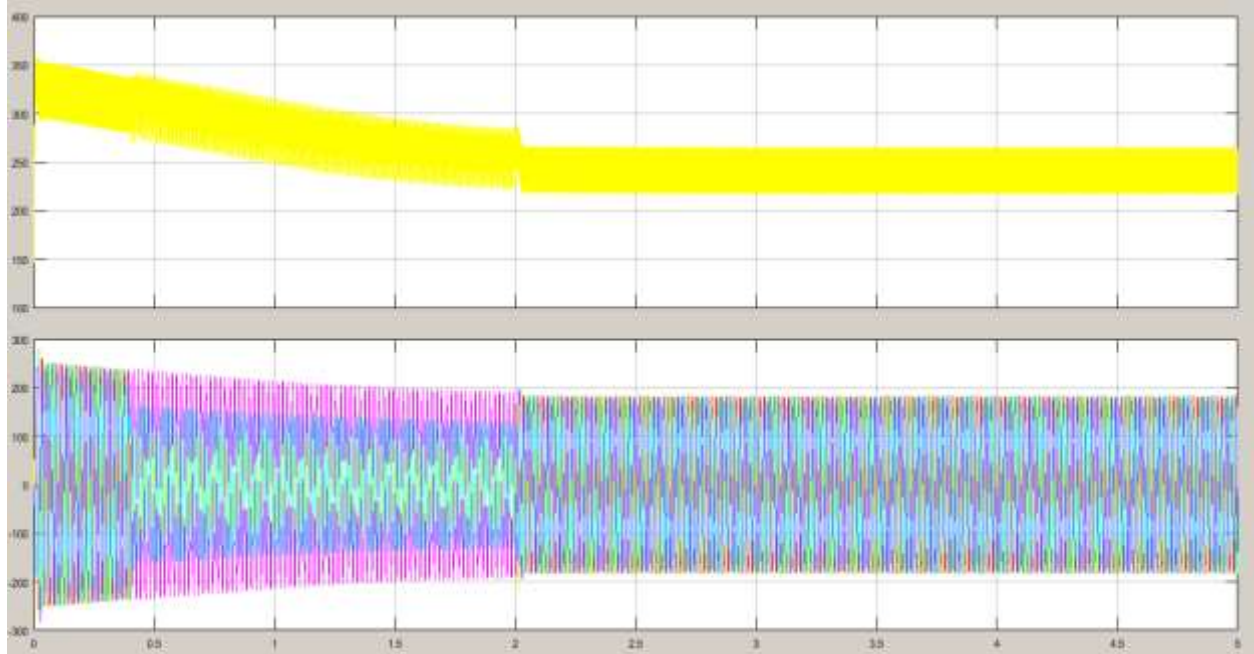


Fig.22. Dc input voltage and three phase grid voltage during case-2

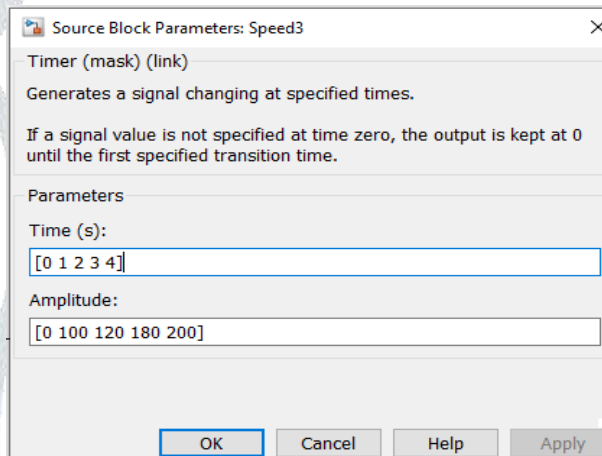


Fig.23. Fuel flow variation with respect to time in second using timer block

Figure 23 shows the timer block in which fuel flow of fuel cell is varies with respect to simulation time. From table, 0 to 1 second fuel flow rate is 0 inch per minute (ipm), 1 to 2 second fuel flow rate is 100 ipm, 2 to 3 seconds fuel flow rate is 120 ipm, 3 to 4 fuel flow rate is 180 ipm and after 4 second fuel flow rate becomes 200 ipm.

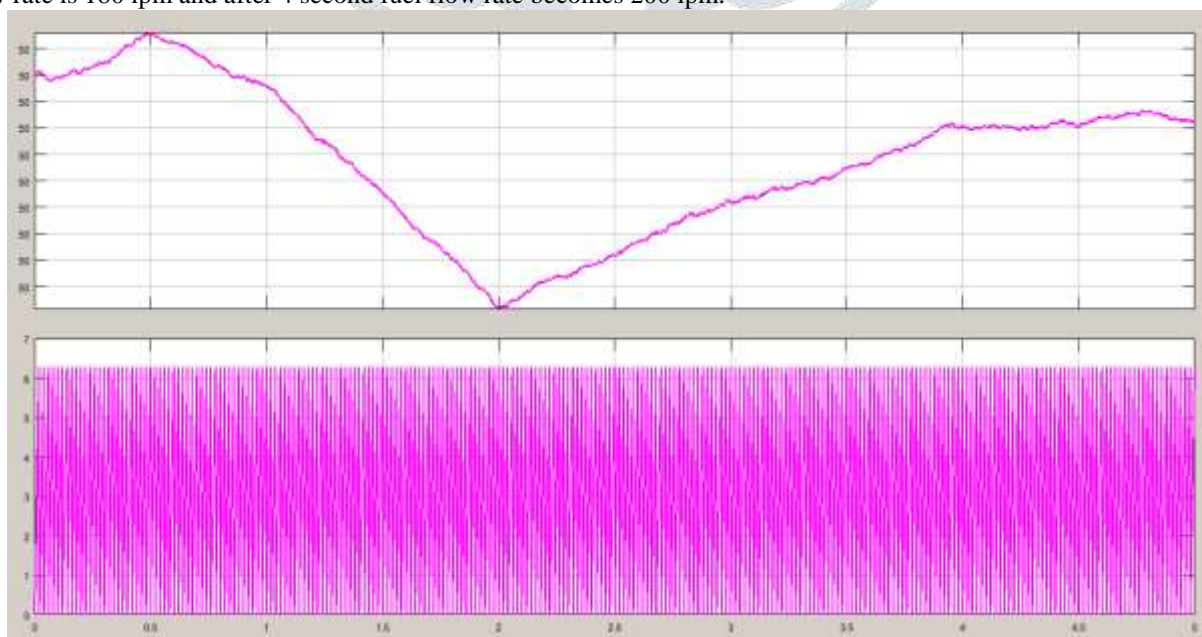


Fig.24. Frequency of system and angular frequency of power system during case-2

Figure 24 shows the supply frequency in Hz and angular frequency of power system during case-2 i.e. constant solar irradiation and variable fuel flow rate. Here it is observe that, supply frequency is constant throughout the operation that is 50 Hz. Where, before 1.5 second simulation time, small fluctuation present in power system frequency which is negligible. Then after 1.5 sec simulation time, frequency of system is constant 50 Hz. Figure 25 shows the Solar PV output DC voltage, Output DC

Current, solar irradiation and temperature during case-2. Here it is observe that, Solar PV output voltage becomes 220 Volts and solar PV current becomes 310 Amp constant throughout the operation. Also solar irradiation becomes 1000 W/m^2 and solar temperature becomes 25 degree Celsius constant throughout the operation under case-2. Figure 26 shows the output DC voltage, DC current, DC generated voltage and DC bus generated current of fuel cell system during case-2. Here, it is observed that, dc output voltage is 70V, fuel system current becomes 5 Amp, DC bus voltage becomes 230 V and DC bus current becomes 100 Amp during case-2.

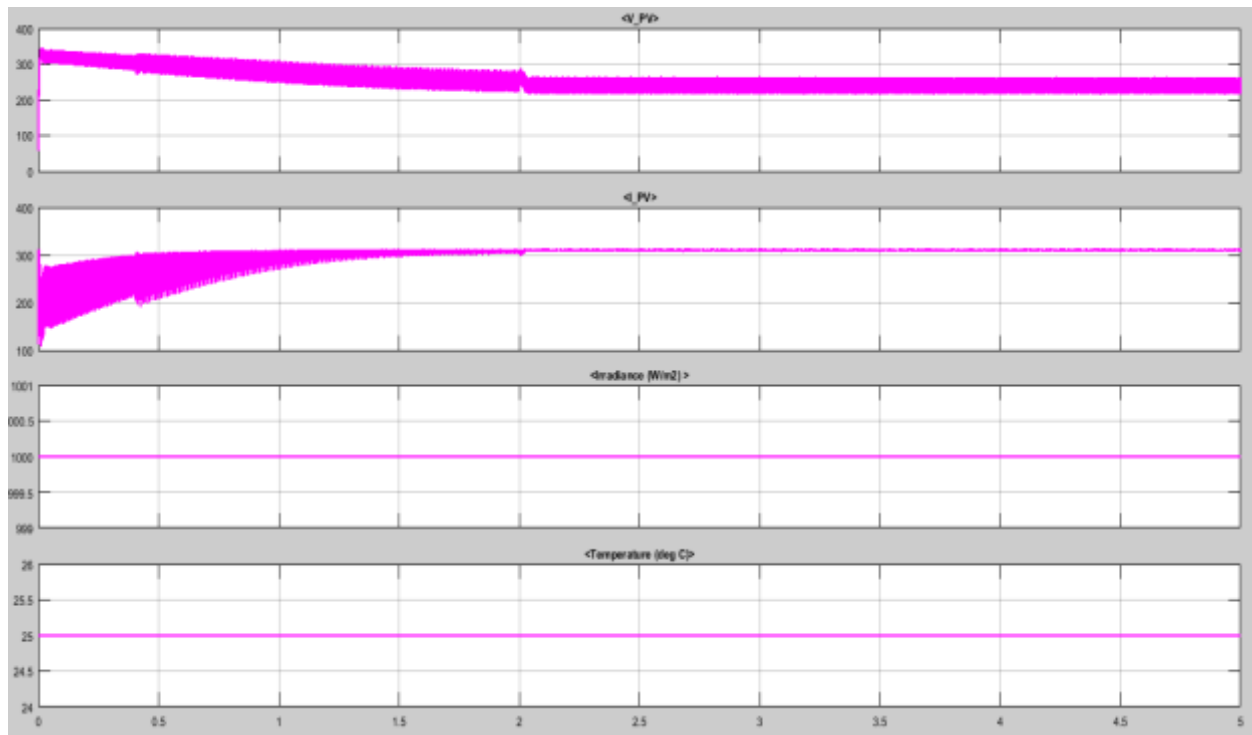


Fig.25. Solar PV output DC voltage, Output DC Current, solar irradiation and temperature during case-2

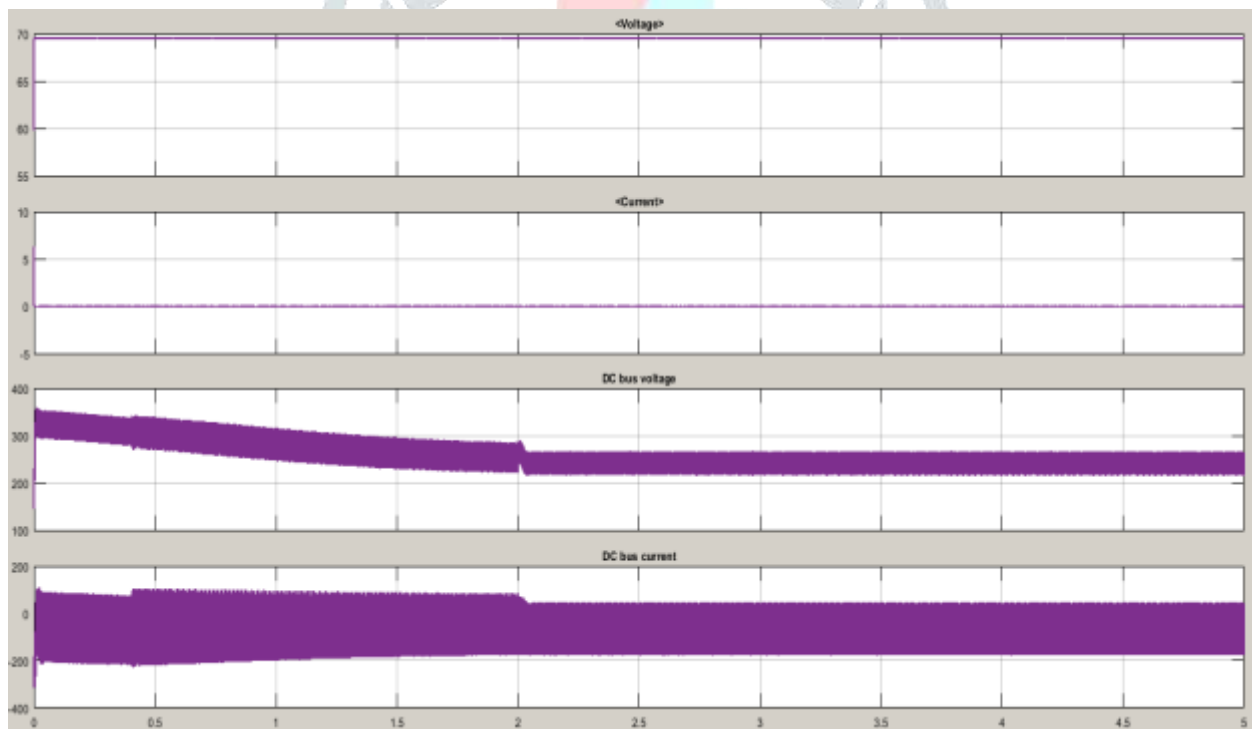


Fig.26. Output DC Voltage, dc current, dc bus generated voltage and dc bus generated current of fuel system during case-2

VI. CONCLUSION

We will present a matlab simulation model for a solar PV system and a fuel battery system in this session. Sim-power system toolbox was used to construct the entire system in MATLAB simulink 2015 programmed. The PV system's results were also analyzed. PV and VI properties of solar pv modules and solar pv array systems were investigated for various solar irradiation and temperature conditions. The outcome of a fuel cell-based battery system analysis. The fuel cell's VI properties, the fuel system's DC output, and the three-phase voltage and current generated by the fuel cell system were all investigated.

As a result, it is apparent that we must build a solar PV and fuel cell battery system that is compatible with a three-phase power grid system. Case-1: Normal condition constant sun irradiation and constant fuel flow rate; case-2: Variable fuel flow rate and constant solar irradiation; and case-3: Variable fuel flow rate and constant solar irradiation. The system was tested in these three instances, and the angular frequency and normal supply frequency were analysed. The angular frequency and supply frequency

are both kept at the permitted level with very minor variations in frequency. As a result, it is apparent that a VSG-based controller power system can sustain system frequency in any circumstance without fluctuation.

REFERENCES

- [1] S. Dierkes, F. Bennewitz, M. Maercks, L. Verheggen, and A. Moser, "Impact of distributed reactive power control of renewable energy sources in smart grids on voltage stability of the power system," in 2014 Electric Power Quality and Supply Reliability Conference (PQ). IEEE, 2014, pp. 119–126.
- [2] U. Tamrakar, D. Shrestha, M. Maharjan, B. Bhattarai, T. Hansen, and R. Tonkoski, "Virtual inertia: Current trends and future directions," *Applied Sciences*, vol. 7, no. 7, p. 654, 2017.
- [3] H. Bevrani, T. Ise, and Y. Miura, "Virtual synchronous generators: A survey and new perspectives," *International Journal of Electrical Power & Energy Systems*, vol. 54, pp. 244–254, 2014.
- [4] A. Vassilakis, P. Kotsampopoulos, N. Hatziaargyriou, and V. Karapanos, "A battery energy storage based virtual synchronous generator," in 2013 IREP Symposium Bulk Power System Dynamics and Control-IX Optimization, Security and Control of the Emerging Power Grid. IEEE, 2013, pp. 1–6.
- [5] J. Liu, Y. Miura, and T. Ise, "Comparison of dynamic characteristics between virtual synchronous generator and droop control in inverterbased distributed generators," *IEEE Transactions on Power Electronics*, vol. 31, no. 5, pp. 3600–3611, 2015.
- [6] J. Alipoor, Y. Miura, and T. Ise, "Stability assessment and optimization methods for microgrid with multiple vsg units," *IEEE Transactions on Smart Grid*, vol. 9, no. 2, pp. 1462–1471, 2016.
- [7] H. Wu, X. Ruan, D. Yang, X. Chen, W. Zhao, Z. Lv, and Q.-C. Zhong, "Small-signal modeling and parameters design for virtual synchronous generators," *IEEE Transactions on Industrial Electronics*, vol. 63, no. 7, pp. 4292–4303, 2016.
- [8] W. Wu, Y. Chen, A. Luo, L. Zhou, X. Zhou, L. Yang, Y. Dong, and J. M. Guerrero, "A virtual inertia control strategy for dc microgrids analogized with virtual synchronous machines," *IEEE Transactions on Industrial Electronics*, vol. 64, no. 7, pp. 6005–6016, 2016.
- [9] C. Andalib-Bin-Karim, X. Liang, and H. Zhang, "Fuzzy-secondarycontroller- based virtual synchronous generator control scheme for interfacing inverters of renewable distributed generation in microgrids," *IEEE Transactions on Industry Applications*, vol. 54, no. 2, pp. 1047–1061, 2018.
- [10] J. Rocabert, A. Luna, F. Blaabjerg, and P. Rodriguez, "Control of power converters in ac microgrids," *IEEE transactions on power electronics*, vol. 27, no. 11, pp. 4734–4749, 2012.
- [11] T. Shintai, Y. Miura, and T. Ise, "Oscillation damping of a distributed generator using a virtual synchronous generator," *IEEE transactions on power delivery*, vol. 29, no. 2, pp. 668–676, 2014.
- [12] A. Fathi, Q. Shafiee, and H. Bevrani, "Robust frequency control of microgrids using an extended virtual synchronous generator," *IEEE Transactions on Power Systems*, vol. 33, no. 6, pp. 6289–6297, 2018.
- [13] K. Sakimoto, Y. Miura, and T. Ise, "Stabilization of a power system including inverter type distributed generators by the virtual synchronous generator," *IEEE Transactions on Power and Energy*, vol. 132, pp. 341–349, 2012.
- [14] Y. Du, J. M. Guerrero, L. Chang, J. Su, and M. Mao, "Modeling, analysis, and design of a frequency-droop-based virtual synchronous generator for microgrid applications," in 2013 IEEE ECCE Asia Downunder. IEEE, 2013, pp. 643–649.
- [15] Y. Hirase, K. Sugimoto, K. Sakimoto, and T. Ise, "Analysis of resonance in microgrids and effects of system frequency stabilization using a virtual synchronous generator," *IEEE Journal of Emerging and Selected Topics in Power Electronics*, vol. 4, no. 4, pp. 1287–1298, 2016.
- [16] C. Li, J. Xu, and C. Zhao, "A coherency-based equivalence method for mmc inverters using virtual synchronous generator control," *IEEE Transactions on Power Delivery*, vol. 31, no. 3, pp. 1369–1378, 2015.